IOSR Journal of Applied Chemistry (IOSR-JAC)
e-ISSN: 2278-5736. Volume 18, Issue 3 Ser. 1 (March 2025), PP 37-48
www.iosrjournals.org

Morphology, Structural and Optical Properties of Nd & Mn doped cobalt nano ferrites by citrate gel auto combustion method

Suryam Neeradi[1], Laxma Reddy Kotha[1*]
[1]*Department of Chemistry, Osmania University, Hyderabad, Telangana, India 500 007*
**Author for correspondence Email: klreddy200542@osmania.ac.in*

Abstract:
To examine the structural and optical properties of nanostructured ferrites, namely those with the formula $Co_{1-y}Mn_yNd_xFe_{2-x}O_4$ x = 0.00, 0.02, 0.04, 0.06, 0.08, and 0.1 nano ferrites, the citrate gel method was employed. X-ray diffraction (XRD) revealed a cubic spinel structure with crystallite diameters ranging from 22 nm to 38 nm; while scanning electron microscopy (SEM) and energy-dispersive X-ray spectroscopy (EDS) revealed the granular morphology and elemental composition. Fourier-transform infrared (FTIR) and Raman spectroscopy were used to describe molecular vibrations, confirming the formation of spinel structures. Optical properties of the samples evaluated by the UV-Visible spectroscopy. Tauc's plots used to calculated optical band gap energy of the samples. The direct band gap energy of the samples found to be range from 1.98 to 2.5 eV.

***Keywords*:** $Co_{1-y}Mn_yNd_xFe_{2-x}O_4$ nano ferrites, X-ray diffraction, FTIR, and Optical properties.

Date of submission: 12-03-2025 Date of acceptance: 26-03-2025

I.Introduction

Nanoferrites are spinel-structured magnetic materials that have special nanoscale characteristics like large surface area, super para magnetism, and adjustable magnetic behaviour. Their versatility in applications such as energy storage, biomedical technology, sensors, and catalysis has led to a great deal of research in material science[1,2]. By using synthesis techniques and doping or changing the composition of their cations, their characteristics can be accurately adjusted. Their magnetic performance and thermal stability are affected by these changes. Spinal ferrites, a class of ceramic magnetic materials with the general formula AB_2O_4, are the subject of much investigation because of their unique structural, catalytic, and magnetic properties[3]. The spinel crystal arrangement is the source of the structure of these materials, while A and B represent different cations, such as divalent and trivalent metal ions, respectively. Within the densely packed cubic lattice of oxygen atoms (O), the cations occupy the interstitial tetrahedral and octahedral sites[4,5]. In a typical spinel ferrite, (A) ions usually occupy tetrahedral sites, while (B) ions occupy octahedral sites, albeit cation inversion may occur depending on the conditions of the material's production[6,7].

These materials' remarkable magnetic permeability and low eddy current losses make them popular for use in inductors, transformers, microwave devices, and magnetic storage. The functional features of nanoferrites are greatly improved by doping them with rare earth or f-block elements, such as Nd, Ce, Y which introduce distinctive electronic configurations and localized magnetic moments[8,9]. These dopants enhance thermal stability, coercivity, and saturation magnetization, which makes the materials perfect for use in spintronic devices and high-density magnetic storage. Furthermore, rare earth ions produce defect states in the bandgap that increase photocatalytic effectiveness and absorption of visible light for the destruction of environmental pollutants.
Rare-earth cations have larger ionic radii than Fe^{3+} or Co^{2+}. When these ions are substituted in the spinel lattice, strain is generated and lattice deformation results. The larger ions disrupt the regular arrangement of the lattice, causing changes in bond lengths and angles, which leads to this strain. Such distortions can affect the material's density, crystallinity, and elastic properties[10].

The induced strain alters the coercivity and magnetic anisotropy of the materials and influences the magnetic interactions between cations at octahedral and tetrahedral sites. The unpaired f-electrons provided by rare-earth ions interact with the d-electrons of the transition metal ions in the spinel structure. This interaction changes the overall magnetic moment of the material[11-13]. Depending on the specific rare-earth ion being used, the magnetic properties, such as saturation magnetization, coercivity, and Curie temperature, can be altered. For instance, the material might be suitable for high-density magnetic storage if the replacement's enhanced anisotropy led to an increase in coercivity[4]. The citrate gel approach is the preferred technique for producing nanoferrites with particular properties for use in biomedical, catalytic, and magnetic applications because of these advantages.

Because of their large surface area, adjustable characteristics, and increased reactivity, nanomaterials are essential for treating water because they effectively remove pollutants such heavy metals, dyes, and pathogens. Nanoferrites are notable among these due to their multifunctionality and magnetic separability[14]. With the use of an external magnetic field, magnetic nanoferrites, such as $ZnFe_2O_4$ or $CoFe_2O_4$, can readily be extracted from treated water and can be used to adsorb heavy metals or break down organic contaminants by photocatalysis. By increasing visible light absorption and decreasing electron-hole recombination, rare earth-doped nanoferrites significantly boost photocatalytic activity and effectively degrade tough contaminants. In addition to increasing treatment effectiveness, these materials provide reusable and sustainable solutions, which are essential for tackling the world's water quality issues. In the present study, synthesized $Co_{1-y}Mn_yNd_xFe_{2-x}O_4$: x = 0.00, 0.02, 0.04, 0.06, 0.08, and 0.1 nano ferrites by citrate gel auto combustion method. The structural, optical and morphological investigations have been done.

II. Experimental analysis

Nano ferrites preparation

$Co_{1-y}Mn_yNd_xFe_{2-x}O_4$ spinel ferrite nanoparticles (x=y = 0.00, 0.02, 0.04, 0.06, 0.08, and 0.1) were synthesized via the "citrate gel auto-combustion method". This method is widely recognized for its simplicity, cost-effectiveness, and ability to produce nanoparticles with uniform combustion and controlled particle size. In this synthesis process, stoichiometric concentrations of metal nitrates, including citric acid, manganese nitrate, ferric nitrate, neodymium nitrate and cobalt nitrate, were dissolved in deionized water. Citric acid act as a chelating agent, forming complexes with metal ions, and also serves as a fuel or combustion agent, which facilitates the auto-combustion process. The pH of the stock solution was adjusted to 7 using ammonia solution, ensuring a neutral environment. The neutral pH was evidenced by the dark green appearance of the solution. The mixture was subjected to continuous stirring at approximately 80 °C on a hot plate, leading to the formation of viscous gel. The gelation process is critical as it allows for uniform distribution of metal ions within the matrix. Upon self-ignition, the gel underwent an exothermic rection, transforming into a highly porous ferrite powder due to the rapid release of gases during the combustion. Subsequently, the resulting powder was subjected to calcination in a muffle furnace at 500ºC for four hours to improve the crystallinity and remove any residual organic matter[15,16]. The calcinated ferrite powder was then finely ground using a mortar and pestle for one hour to achieve a uniform particle size and enhance its magnetic properties. **Fig 1.** Shows the flow chart of citrate gel auto combustion method.

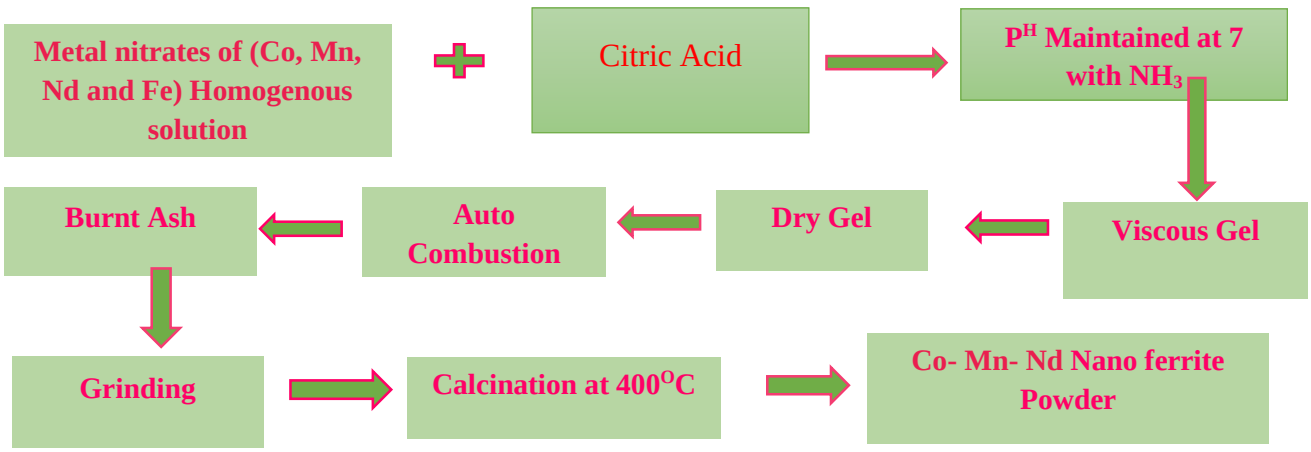

Fig. 1. Flow chart of Co-Mn-Nd nano ferrites synthesis

Material Characterization Techniques

$Co_{1-y}Mn_yNd_xFe_{2-x}O_4$ (x,y= 0.00-NdMN-0, 0.02-NdMN-1, 0.04-NdMN-2, 0.06-NdMN-3, 0.08-YbMN-4, and 0.1-NdMN-5) nanoparticles were subjected to X-ray diffraction utilizing a Bruker D-8 advanced and an X-ray diffractometer with Cu Kα radiation at 0.15406 nm in order to determine their spinel-phase and cubic nature. To analyse the morphology, a field emission scanning electron microscope (FE-SEM, JEOL JSM-6480LV) and energy dispersive spectroscopy (EDS) were employed. The materials' spinel phase development can be verified using a laser FTIR (FTIR-PerkinElmer L1600). A Shimadzu UV-NIR UV-3600 Plus double beam spectrophotometer was used to analyse the spectral band gap of Mn & Nd-substituted CoFe2O4. A VSM has been used to assess the magnetism of the prepared sample (VSM-Quantum Design, USA, PPMS-DynaCool-9T). A UV–vis spectrophotometer (UVS-2800, USA) was used to detect the degradation of MB, and acid red, the absorbance of the irradiated mixture was determined at different times.

Materials photocatalytic activity

The photocatalytic activity of the prepared samples was evaluated using two dyes that are sensitive to visible light: Methylene Blue (MB) and Rhodamine Blue (RB). For the experiment, 0.05 g of both MB and acid red were carefully weighed and set aside. Similarly, 0.05 g of the catalyst, specifically the ferrite sample, was separately measured and dissolved in deionized distilled (DD) water. To ensure uniform dispersion, each dye and catalyst were independently dissolved in approximately 50 millilitres of DD water. The solutions were then thoroughly mixed using a magnetic stirrer to achieve homogeneity. Before exposing the samples to light irradiation, the mixtures were kept in the dark for 20 minutes to establish adsorption equilibrium between the dye molecules and the catalyst surface. A 400 W power bulb was utilized as the irradiation source to simulate visible light conditions. During the photocatalytic experiment, samples were extracted at specific time intervals using a 20-gauge syringe. In this case, the time intervals were fixed at every 20 minutes to monitor the degradation process systematically.

III. Results and Discussions

XRD analysis

X-ray diffraction technique is a prime significant technique for analysing the phase and crystalline nature of the materials. **Fig. 2** indicates the X-ray diffraction pattern of the synthesized $Co_{1-y}Mn_yNdxFe_{2-x}O_4$ x=y = 0.02, 0.04, 0.06, 0.08, and 0.1 nano ferrites. X-ray diffraction pattern of the synthesized ferrites samples indicated a single-phase cubic spinel structure and the absence of secondary phase[17,18]. The XRD pattern planes well matched indexed include the 111, 220,311, 222, 400, 422, 511, and 440. The x-ray diffraction pattern planes well matched with JCPDS card number 001-1121; the measured XRD peaks indexed with a cubic spinel structure.

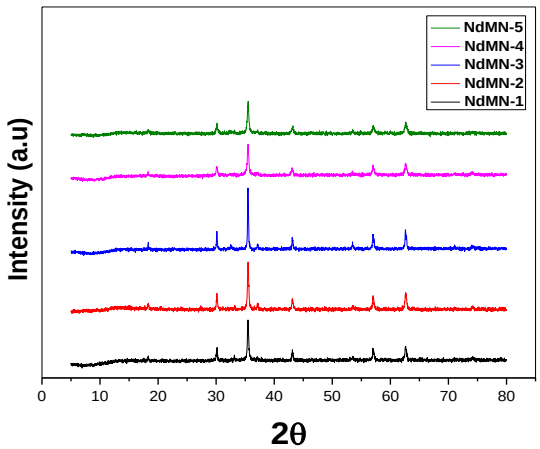

Fig.2 X-ray diffraction pattern of $Co_{1-y}Mn_yNd_xFe_{2-x}O_4$ x = 0.02, 0.04, 0.06, 0.08, and 0.1 nano ferrites

The prepared Nd & Mn substituted cobalt based nano ferrites exhibit a crystalline nature with Fd3m space group and FCC structure, highlighting the samples asymmetry and stability[19]. Additionally, the XRD pattern of the prepared samples indicates the absence of secondary phase or contaminants. From the broad and high intensity peaks, the average crystalline size of the samples was calculated by the following Debye-Scherrer equation[20].

$$Crystalline\ size\ (D) = \frac{0.94\lambda}{\beta COS\theta}$$

The lattice parameter of the samples was calculated by following equation. $Lattice\ parameter\ a = d\sqrt{h^2 + k^2 + l^2}$. where d indicates interplanar distance and h, k, and l indicates miller indices. The average crystalline size and lattice parameter of $Co_{1-y}Mn_yNd_xFe_{2-x}O_4$ nano ferrites with x = 0.02, 0.04, 0.06, 0.08, and 0.1 vary, as shown in **Fig. 3**. The average crystalline size of the Co-Mn-Nd nano ferrites was found to be in the range of 22-38 nm, while the lattice parameter of the samples ranged from 8.366 to 8.381 Å. The crystalline size of the samples initially decreased up to a concentration x=y=0.04. Later it increased to a higher value around 37 nm before gradually decreasing again 22 nm. The similar trend was observed in the lattice constant of the synthesized samples. This variation of the synthesized spinel ferrites indicates that the unit cell size has been altered by the structural changes like ionic substitution, lattice strain or preparation. Substituting metal cations with different ionic radii may alter both properties. The following equation was used to calculate the unit cell volume of the samples. $Volume\ of\ unit\ cell\ (v) = a^3$.

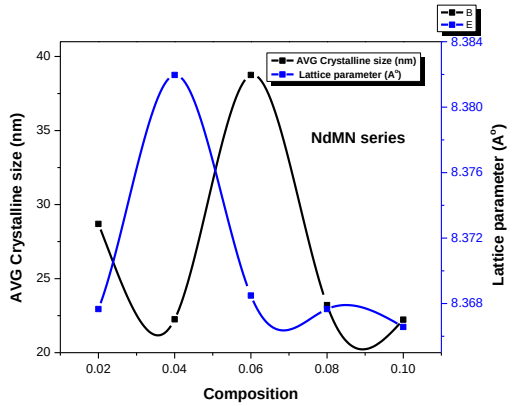

Fig.3 Variation of crystalline size and Lattice parameter of $Co_{1-y}Mn_yNd_xFe_{2-x}O_4$ x = 0.0, 0.02, 0.04, 0.06, 0.08, and 0.1 nano ferrites

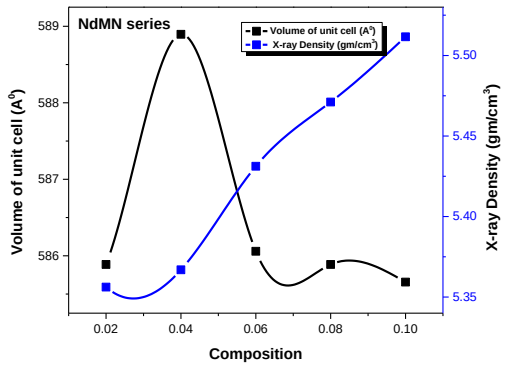

Fig.4 Volume of unit cell and X-ray density of $Co_{1-y}Mn_yNd_xFe_{2-x}O_4$ x = 0.0, 0.02, 0.04, 0.06, 0.08, and 0.1 nano ferrites

Table 1. XRD parameters of $Co_{1-y}Mn_yNd_xFe_{2-x}O_4$ x = 0.0, 0.02, 0.04, 0.06, 0.08, and 0.1 nano ferrites

S.no	Name of the composition	Peak position(2ɵ) (degree)	FWHM(β)	Avg crystalline size(nm)	Lattice parameter(A^0)	Volume of unit cell(A^0)	X-ray density (g/mm^3)
1	NdMN-1	35.490	0.274	28.69	8.367	585.886	5.35
2	NdMN-2	35.428	0.354	22.25	8.381	588.895	5.36
3	NdMN-3	35.487	0.203	38.75	8.368	586.059	5.43
4	NdMN-4	35.490	0.339	23.21	8.367	585.886	5.47
5	NdMN-5	35.495	0.354	22.22	8.366	585.655	5.51

The calculated unit cell volume varied between 585.88 to 588.89 Å, suggesting that the addition of Nd to the host material caused minor changes. These variations in lattice parameter and unit cell volume can be due to substitutional insertion of Nd and Mn, strain effects, or small crystal lattice distortion. **Fig. 4** indicates the variation of volume of unit cell and X-ray density of the prepared $Co_{1-y}Mn_yNd_xFe_{2-x}O_4$ x = 0.0, 0.02, 0.04, 0.06, 0.08, and 0.1 nano ferrites.

FE-SEM and EDS of Nd-Mn-Co nano ferrites

Field emission scanning electron microscope (FESEM) is crucial to nano science, particularly, for the analyse the characterization of spinel nano ferrites. These powerful images technique provides thorough insights into the surface morphology of nano materials, enabling researcher to investigate particles sizes, shapes and aggregation. This Knowlagent is significance since these parameters directly affect the functional and physical properties of nano ferrites. **Fig. 5** illustrates the FESEM images of $Co_{1-y}Mn_yNd_xFe_{2-x}O_4$ nano ferrites with x =y= 0.0, 0.02, 0.04, 0.06, 0.08, and 0.1. All the synthesized samples FE-SEM images show spherical and cluster type. FESEM images of the samples of the grains are arranged in agglomeration[21–23]. This behaviour is caused by higher interparticle magnetic interactions and grain formation, which are commonly observed in doped ferrites.

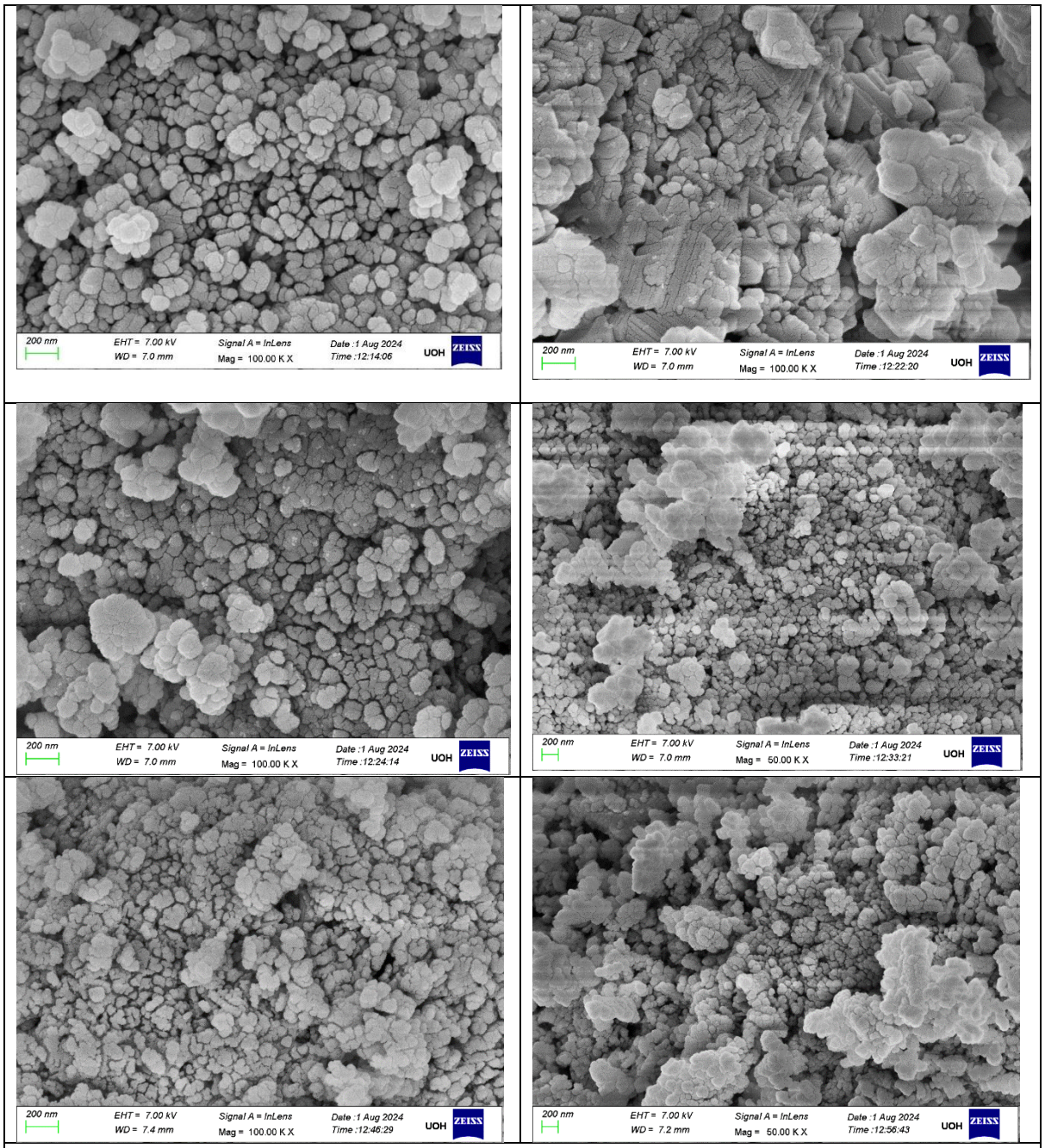

Fig.5 FE-SEM images of $Co_{1-y}Mn_yNd_xFe_{2-x}O_4$ x = 0.0, 0.02, 0.04, 0.06, 0.08, and 0.1 nano ferrites

Energy dispersive spectroscopy is a significant tool for determining the elemental and atomic content of the materials. The synthesized $Co_{1-y}Mn_yNd_xFe_{2-x}O_4$ x = 0.0, 0.02, 0.04, 0.06, 0.08, and 0.1 nano ferrites are analysed using EDS, indicated in **Fig. 6**. The EDAX spectrum of the samples provide comprehensive elemental insights, which are essential for comprehending and improving these materials. The resultant EDS graphs show both qualitative and quantitative data of the spinel nano ferrites. The spectrum graphs confirm the presence of Fe, O, Mn, Co, and Nd elements according to stoichiometric ratio. The EDS spectrum further confirms the successful incorporation of Co, Mn, Nd and Fe in the ferrite's samples. The Nd and Mn metal intensities increases as the doping concentration increases, indicating successful substitution. Additionally, the presence of Co, Fe, Mn and Nd of the spectrum suggests that the composition remains stable with Mn and Nd doping.

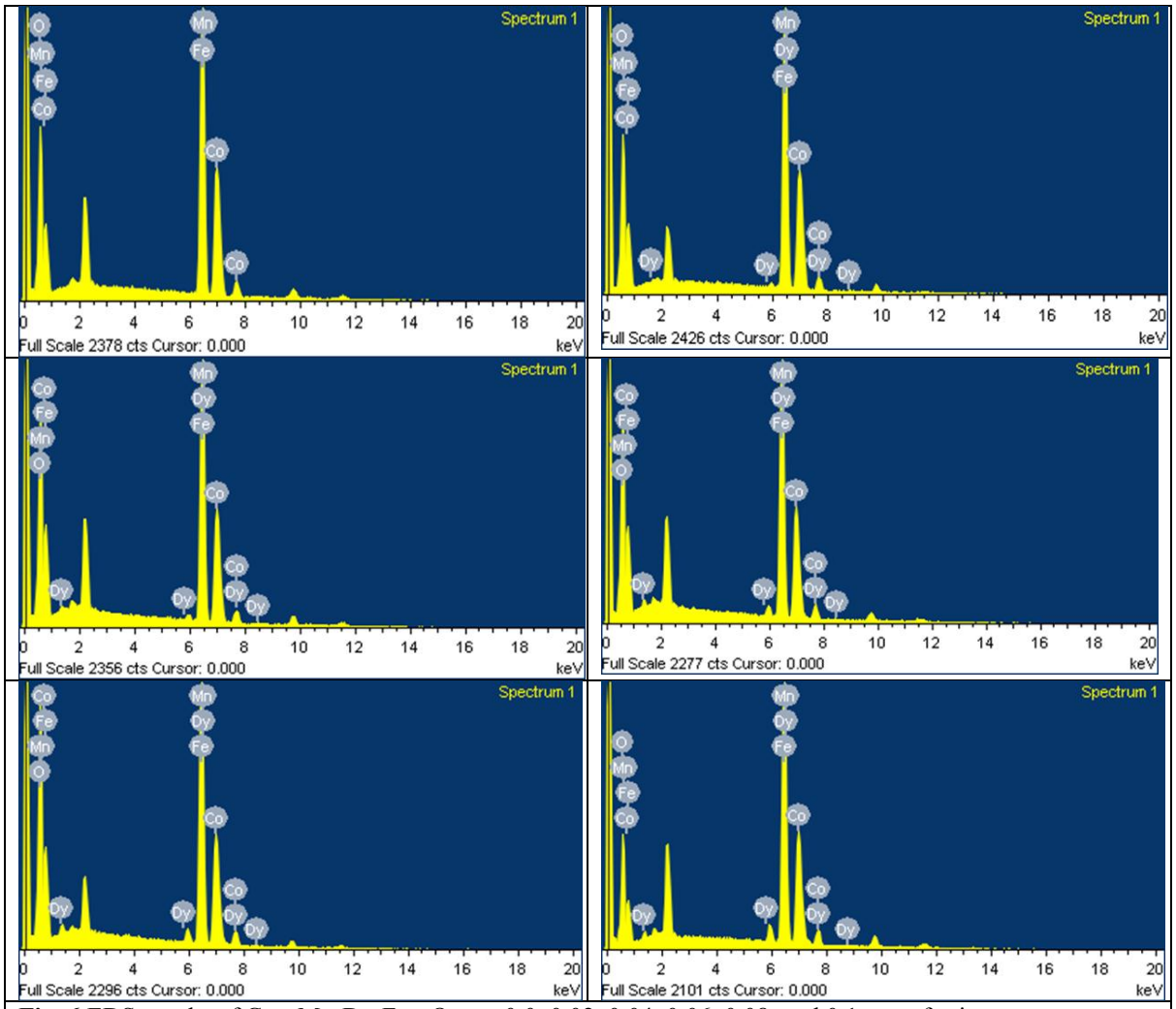

Fig. 6 EDS graphs of $Co_{1-y}Mn_yDy_xFe_{2-x}O_4$ x = 0.0, 0.02, 0.04, 0.06, 0.08, and 0.1 nano ferrites

FTIR spectrum of Nd-Mn-Co nano ferrites

The FTIR spectroscopy is an analytical tool used to determine the functional groups present in the synthesized materials. Additionally, it provides insight into the molecular interactions within the materials. The FTIR spectrum also reveals the vibrational modes of chemical bonds in the fingerprint region, offering valuable information about the bonding nature, crystallinity, and structure of the nano materials particularly nano ferrites. Fig 7 indicates the FTIR spectrum of the prepared $Co_{1-y}Mn_yNd_xFe_{2-x}O_4$ where x, y = 0.0, 0.02, 0.04, 0.06, 0.08, and 0.1 nano ferrites. The vibrations spectrum exhibits two distinct FTIR bands associated with octahedral and tetrahedral sites within the 400 to 600 cm-1 wavenumber domains. These sites play a significant role in the structural characterization of nano materials. The FTIR bands observed around 400 to 500 cm-1 domains associated to the stretching vibrations of metal oxygen bonds (M-O linkage) at octahedral sites. Another FTIR band, appearing at 500 to 600 cm-1 wavenumber domain corresponds to the stretching symmetrical vibrations metal cations with oxygen bond linkage of tetrahedral sites[24]. The presence of both octahedral and tetrahedral bands in the synthesised samples confirms the formation of a spinel structure.

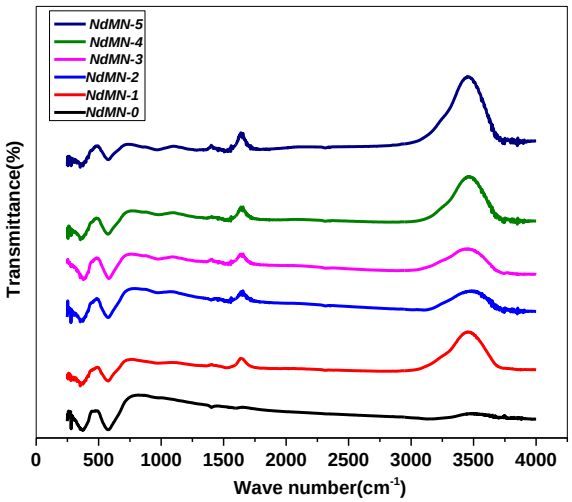

Fig. 7 FTIR spectrum of $Co_{1-y}Mn_yNd_xFe_{2-x}O_4$ x = 0.0, 0.02, 0.04, 0.06, 0.08, and 0.1 nano ferrites

Raman spectrum of Nd-Mn-Co nano ferrites

Raman spectroscopy is a significant method to examining the vibrational and structural characterization of nano materials, particularly nano ferrites. The materials phase composition, cation distribution, and lattice constant of the nano ferrites could be thoroughly explained by it. The characteristic Raman active vibrational modes of nano ferrites, which often exhibit spinel structures, correlate to the stretching and bending of metal oxygen bonds in tetrahedral and octahedral sites. Additionally, it can distinguish between distinct ferrite phases and identify impurities or secondary phases. The $Co_{1-y}Mn_yNd_xFe_{2-x}O_4$ where x, y = 0.0, 0.02, 0.04, 0.06, 0.08, and 0.1 spinel nano ferrites shown in Fig.8, exhibit Raman spectrum with strong bands in the lower wavenumber region, which are suggestive of vibrational modes related to the lattice dynamics of spinel ferrites. These bands indicate the stretching and bending vibrations of metal-oxygen bonds, which are commonly seen in spinel structures[25]. The symmetrical stretching and asymmetric bending vibrations of tetrahedral (A-site) and octahedral (B-site) environments, respectively, are responsible for the peaks located between 200 to 800 cm-1. The observed intensity variations and minor shifts across the samples suggest changes in local structural symmetry or cation distribution due to different compositions. Five Raman bands observed in the spectrum, attributed to the A2g, Eg, and 3T2g modes, are predicted by group theory representation for the spinel structure, which belongs to the Fd3m space group. Nd and Mn doped probably modifies bond lengths and cation occupancy, which impacts the lattice symmetry and shifts vibrational frequencies.

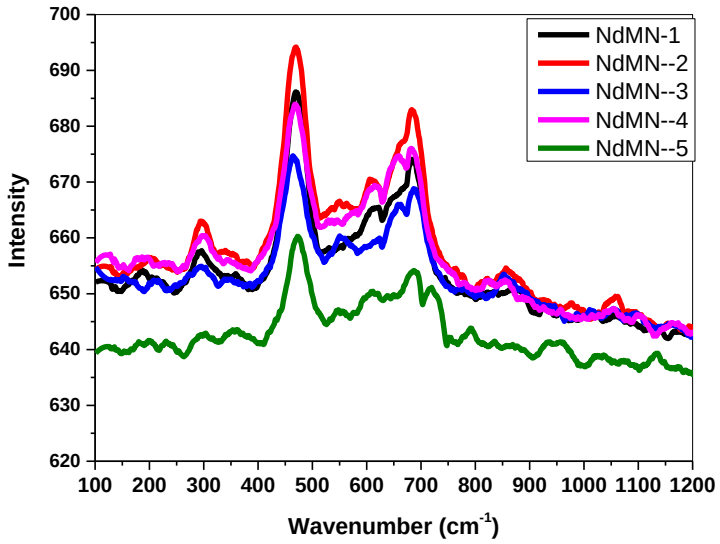

Fig.8 Raman spectrum of $Co_{1-y}Mn_yNd_xFe_{2-x}O_4$ x = 0.0, 0.02, 0.04, 0.06, 0.08, and 0.1 nano ferrites

Optical spectroscopic features of Nd series

A material's reaction to electromagnetic radiation or incoming light is a fascinating phenomenon given the prevalence of modern applications. In this optical studies Nd and Mn substituted cobalt based nano ferrites was investigated for various applications. Tauc's and Urbach's relations were used to assist in the absorbance-based analysis [24]. The thickness and absorbance values are used to calculate the optical absorption coefficient, or "α." The "α" has been calculated using the relation below as

$$\alpha = 2.303 * \frac{\text{Absorbance}}{Thickness\ of\ the\ sample}$$

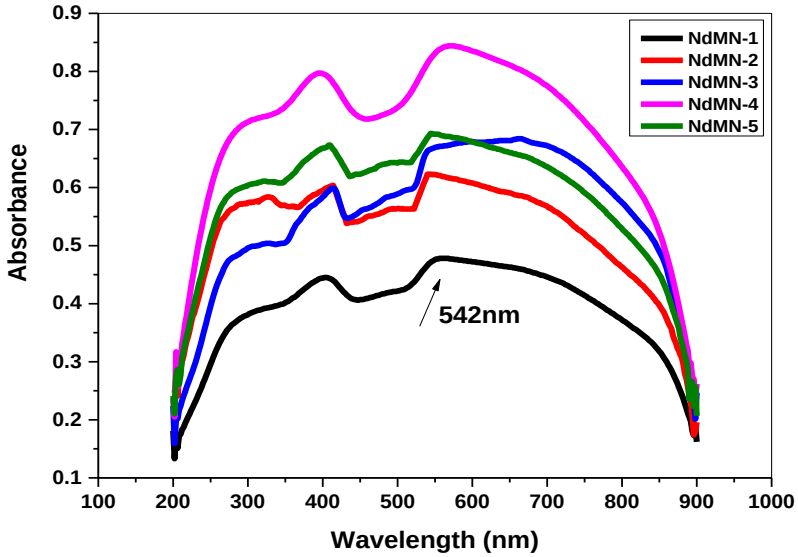

Fig.10 UV-Optical spectra of Neodymium and Manganese doped cobalt nano ferrites

Fig. 10 shows the absorbance varies with the UV light wavelength impinge on the Nd & Mn-doped cobalt NFs under study. The thickness based optical absorbance variation with wavelength was recorded. Due to insertion of the dopant Nd into the ferrite composition, the optical characteristics of the samples have changed. It is evident that the dopant concentration affects the cut-off edge. Among the series of samples with varying dopant concentrations, the cut-off for the pure sample Nd-0 was determined to be the highest (542 nm). It could happen as a result of the nano ferrites' altered structure when the dopant is substituted into the base matrix. The octahedral sites are preferred by rare earth oxides such as La, Tm, and Nd, and they can occasionally occupy both the Oh and Th sites of the base ferrite. The cut-off wavelength or cut-off frequency varies with a decreasing trend between 542 and 518 nm.

Table 2. Optical parameters of $Co_{1-y}Mn_yNd_xFe_{2-x}O_4$ x = y= 0.02, 0.04, 0.06, 0.08, and 0.1 nano ferrites

Sample code	Cut-off wavelength (nm)	Indirect band gap(eV)	Direct band gap(eV)	Urbach energy (eV)	Refractive index (n)	Dielectric constant
NdMN-1	542	2.10	1.98	0.75	2.24	5.01
NdMN-2	534	2.22	2.16	0.78	2.32	5.38
NdMN-3	530	2.34	2.30	0.85	2.40	5.76
NdMN-4	525	2.42	2.40	0.90	2.44	5.95
NdMN-5	518	2.58	2.50	0.96	2.48	6.15

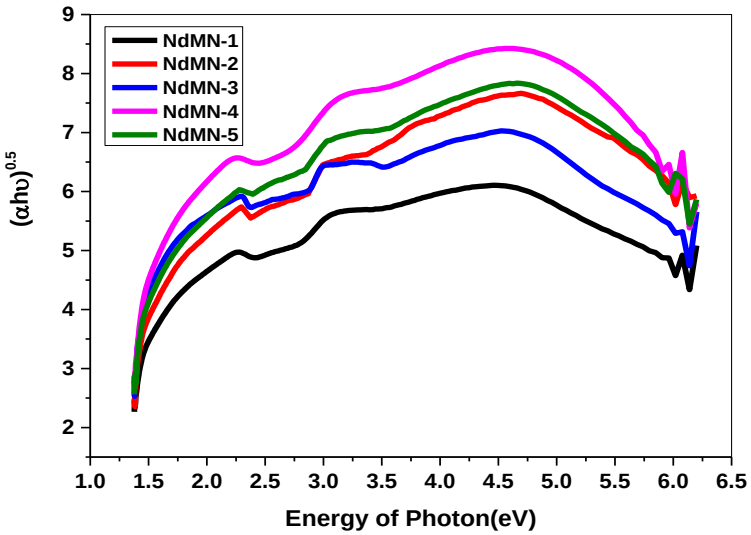

Fig.11 Taucs relation for indirect band gap of Neodymium and Manganese doped cobalt nano ferrites

The Tauc's technique is a good estimate for determining the direct and indirect band gap of the material. The variation of (hαυ) 0.5 with the photon incidence energy is seen in **Fig. 11.** The indirect-band gap energy can be thought of as the curve where the point crosses the X-axis. The band gap (E indirect) value of the Nd & Mn doped cobalt NFs in the current work is 2.10 eV. Additionally, it rose in a systematic way as Nd was doped into the base matrix. The Nd-5 sample had the highest value, 2.58 eV. The conversion of structural variations as a result of the addition of Nd content could be the cause. For both direct and indirect bandgaps, the Taucs connection can be displayed as follows.

$$(h\alpha\upsilon)^{1/k} = C(h\upsilon - Eg)$$

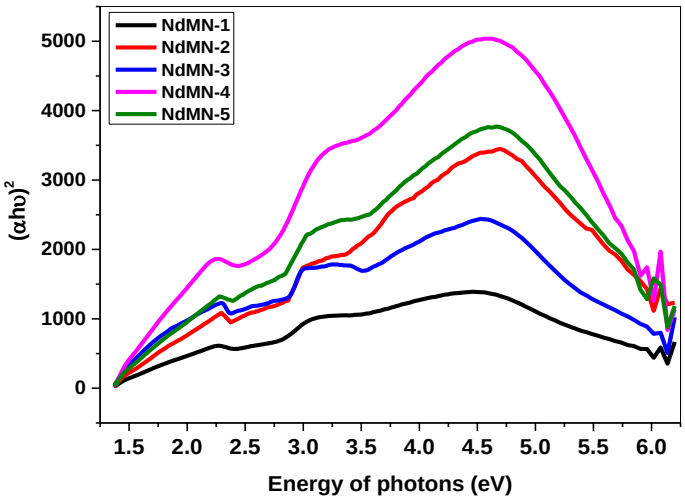

Fig.12. Taucs relation for direct energy band gap of Neodymium and Manganese doped cobalt nano ferrites

The variation in $(h\alpha\upsilon)^2$ with photon incidence energy is shown in **Fig. 12**. The direct-band gap energy, which is more suited for ferrite compositions, may be shown by the curves where the point cuts the X-axis. The current study's series of Nd & Mn -doped cobalt-based NFs revealed a band gap (E direct) value of 1.98 eV. Additionally, it rose in a systematic way as Nd was doped into the base matrix[26,27]. The Nd-5 samples had the highest value, 2.50 eV. The conversion of structural variations as a result of adding Nd content could be the cause.

Urbach Energy (E_{Urbach}) calculation:
Urbach energy is an associated parameter with randomness of the materials. It also depends on the absorption coefficient as shown in the following relation

$$\ln(\alpha) = \ln(\alpha_0) + \left(\frac{hv}{E_{Urbach}}\right)$$

The order of randomness created in the material as a result of dopant addition is measured by the ΔE scale. The absorption coefficient's change with photon energy, which yields the Urbach energy value, is shown in **Fig. 13**. With a step of 0.02, it changed linearly from 0 to 0.1 as a function of dopant concentration in the current method. The change of ΔE between 0.75eV and 0.96V provides further evidence that the dopants increase the degree of unpredictability in the structure of the base ferrite composition.

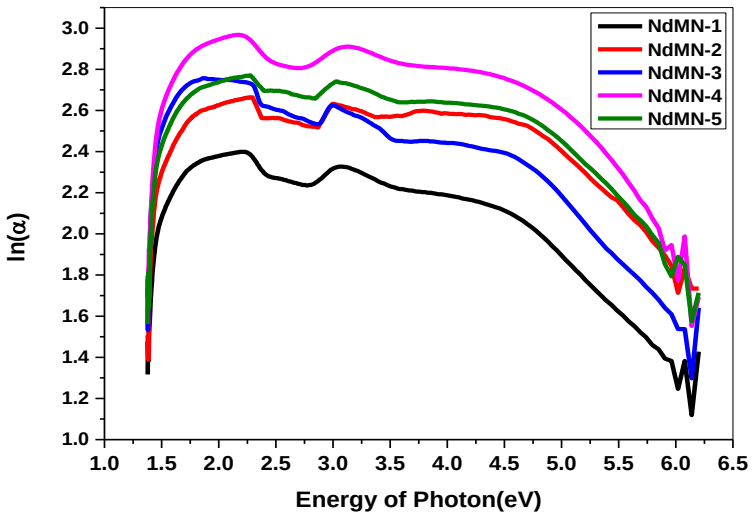

Fig.13 Urbach Energy (E_{Urbach}) calculation of Neodymium doped Co-Mn nano ferrites

Refractive index (μ)
Using the direct band gap energy value, the refractive index was calculated from Tauc's relation. The parameter is the only determinant of the application-oriented approach and optical stability. The Neodymium doped NFs' refractive index rose linearly with the dopant. It showed a linear increase and ranged from 2.24-2.48. The square of the refractive index is the optical dielectric constant.

IV.Conclusions

- Mn and Nd doped cobalt based nano ferrites were successfully synthesized using the citrate gel method, forming a well-defined cubic spinel phase.
- The structural characterization using X-ray diffraction (XRD) confirmed the formation of a cubic spinel structure, with crystallite sizes ranging between 22 nm and 38 nm.
- The lattice parameter and unit cell volume showed slight variations due to the incorporation of Mn and Nd, indicating structural distortions.
- Field emission scanning electron microscopy (FESEM) revealed a spherical and clustered morphology, while energy dispersive spectroscopy (EDS) verified the elemental composition and confirmed the successful incorporation of the dopants.
- Fourier-transform infrared (FTIR) and Raman spectroscopy provided insights into the vibrational properties and confirmed the presence of both tetrahedral and octahedral sites in the spinel structure.
- Optical studies using UV-Visible spectroscopy demonstrated that the direct band gap energy of the materials ranged between 1.98 eV and 2.50 eV, with a systematic increase observed as the dopant concentration increased.
- The structural analysis confirmed lattice distortions due to doping, while optical characterization showed a tunable band gap with increasing dopant concentration.

Acknowledgement

Authors are thankful to Department of Chemistry, UCS, O.U, Hyderabad for provided necessary facilities to carry out the research work.

References

[1] R.M. Kershi, A.M. Alshehri, R.M. Attiyah, Enhancement of Ni–Zn ferrite nanoparticles parameters via cerium element for optoelectronic and energy applications, Discover Nano 18 (2023). https://doi.org/10.1186/s11671-023-03921-6.

[2] M.A. Abdo, R. Al-Wafi, M.S. AlHammad, Highly efficient visible light driven photocatalytic activity of rare earth cerium doped zinc-manganese ferrite: Rhodamine B degradation and stability assessment, Ceram Int 49 (2023). https://doi.org/10.1016/j.ceramint.2023.06.213.

[3] M. Sajjad, K. Ali, Y. Javed, A. Sattar, L. Akbar, A. Nawaz, M.Z. Rashid, K. Rasool, M. Alzaid, Detailed analysis of structura1 and optical properties of spinel cobalt doped magnesium zinc ferrites under different substitutions, Journal of Materials Science: Materials in Electronics 31 (2020). https://doi.org/10.1007/s10854-020-04690-z.

[4] M. Kaiser, Effect of rare earth elements on the structural, magnetic and electrical behavior of Ni-Zn-Cr nanoferrites, J Alloys Compd 719 (2017). https://doi.org/10.1016/j.jallcom.2017.05.155.

[5] E. Ateia, A.A.H. El-Bassuony, Fascinating improvement in physical properties of Cd/Co nanoferrites using different rare earth ions, Journal of Materials Science: Materials in Electronics 28 (2017). https://doi.org/10.1007/s10854-017-6944-0.

[6] M. Hashim, A. Ahmed, S.A. Ali, S.E. Shirsath, M.M. Ismail, R. Kumar, S. Kumar, S.S. Meena, D. Ravinder, Structural, optical, elastic and magnetic properties of Ce and Dy doped cobalt ferrites, J Alloys Compd 834 (2020). https://doi.org/10.1016/j.jallcom.2020.155089.

[7] M.N. Akhtar, Z.M. Elqahtani, S. Qamar, A. Almohammedi, M. Irfan, M.A. Khan, M. Yousaf, A. Nazir, Y. Lu, M.Z. Mahmoud, M. Aslam, Z.A. Alrowaili, M.S. Al-Buriahi, Microwave absorption, physicochemical, elemental mapping, and high-frequency perspectives of the Co, Cu, Zn doped Ni-Ce absorbers for Ku band frequency, Surfaces and Interfaces 42 (2023). https://doi.org/10.1016/j.surfin.2023.103377.

[8] N.M. Basfer, N. Al-Harbi, Structural, optical and photocatalytic activity of Ce3+ doped Co–Mg nanoparticles for wastewater treatment applications, J King Saud Univ Sci 35 (2023). https://doi.org/10.1016/j.jksus.2022.102436.

[9] S. K.A.Ahamed, V. Naidu, S. Amalorpava Mary, S. Vijay Anand, Magnetic Property Study of Nickel Cerium Doped Zinc Ferrite Nano Particles, Int J Comput Appl 40 (2012). https://doi.org/10.5120/5030-7180.

[10] S. Raghuvanshi, F. Mazaleyrat, S.N. Kane, Mg1-xZnxFe2O4 nanoparticles: Interplay between cation distribution and magnetic properties, AIP Adv 8 (2018). https://doi.org/10.1063/1.4994015.

[11] K.J. Wadi, H.A. Abbas, A.H. Ali, B.M. Hasan, A study of micro structural, magnetic and electrical properties of La-Co-Sm nanoferrites (LCSF) synthesized by sol-gel method, International Journal of Electrical and Computer Engineering 10 (2020). https://doi.org/10.11591/ijece.v10i2.pp1772-1781.

[12] V. Naidu, S.K.A. Ahamed Kandu Sahib, M. Sivabharathy, R. Legadevi, A.S. Kumar, C. Prakash, S. Pandian, Synthesis and characterization of novel nano ceramic magnesium ferrite material doped with samarium and dysprosium for designing-microstrip patch antenna, Defect and Diffusion Forum 332 (2012). https://doi.org/10.4028/www.scientific.net/DDF.332.35.

[13] M.A. Ahmed, N. Okasha, A.A. Mohamed, I. Mmdouh, Optimizing the structure and magnetic properties of SmCo nanoferrites synthesized by auto-combustion processing techniques, J Magn Magn Mater 358–359 (2014). https://doi.org/10.1016/j.jmmm.2013.12.027.

[14] S. Kumari, N. Dhanda, A. Thakur, V. Gupta, S. Singh, R. Kumar, S. Hameed, P. Thakur, Nano Ca–Mg–Zn ferrites as tuneable photocatalyst for UV light-induced degradation of rhodamine B dye and antimicrobial behavior for water purification, Ceram Int 49 (2023). https://doi.org/10.1016/j.ceramint.2022.12.107.

[15] R. Sato Turtelli, G. V. Duong, W. Nunes, R. Grössinger, M. Knobel, Magnetic properties of nanocrystalline CoFe2O4 synthesized by modified citrate-gel method, J Magn Magn Mater 320 (2008). https://doi.org/10.1016/j.jmmm.2008.02.067.

[16] C.D. Viet, N.T. Nga, D.D. Tho, T.V.D. Ngoc, N. Van Dung, L.H. Bac, STRUCTURAL, ELECTRICAL AND FERROELECTRIC PROPERTIES OF NiTiO3 NANOPARTICLES SYNTHESIZED BY CITRATE-GEL METHOD, Vietnam J Sci Technol 60 (2022). https://doi.org/10.15625/2525-2518/16212.

[17] M.M. El-Masry, R. Ramadan, The effect of CoFe2O4, CuFe2O4 and Cu/CoFe2O4 nanoparticles on the optical properties and piezoelectric response of the PVDF polymer, Appl Phys A Mater Sci Process 128 (2022). https://doi.org/10.1007/s00339-021-05238-6.

[18] A. Kalam, A.G. Al-Sehemi, M. Assiri, G. Du, T. Ahmad, I. Ahmad, M. Pannipara, Modified solvothermal synthesis of cobalt ferrite (CoFe2O4) magnetic nanoparticles photocatalysts for degradation of methylene blue with H2O2/visible light, Results Phys 8 (2018). https://doi.org/10.1016/j.rinp.2018.01.045.

[19] B.A. Patil, R.D. Kokate, Synthesis and Design of Magnetic Parameters by Ti doping in Cobalt Ferrite Nanoparticles for Nanoelectronics Applications, in: Procedia Manuf, 2018. https://doi.org/10.1016/j.promfg.2018.02.021.

[20] E. Sumalatha, M. Nyathani, T.A. Babu, D. Ravinder, N.V.K. Prasad, S. Katlakunta, Eco-friendly synthesis, TEM and magnetic properties of Co-Er nano-ferrites, Biointerface Res Appl Chem 12 (2022). https://doi.org/10.33263/BRIAC121.910928.

[21] P.A. Asogekar, V.M.S. Verenkar, Structural and magnetic properties of nanosized CoxZn(1-x)Fe2O4 (x= 0.0, 0.5, 1.0) synthesized via autocatalytic thermal decomposition of hydrazinated cobalt zinc ferrous succinate, Ceram Int 45 (2019). https://doi.org/10.1016/j.ceramint.2019.07.182.

[22] P.N. Dave, R. Sirach, An Efficient Nanocatalyst Cobalt Copper Zinc Ferrite for the Thermolysis of Ammonium Nitrate, ACS Omega 7 (2022). https://doi.org/10.1021/acsomega.2c04796.

[23] N. Desai, Y.N. Sudhakar, R.R. Patil, A. Chandran, M. Nidhin, A.S. Agnihotri, Electrochemical sensor based on PVP coated cobalt ferrite/graphite/PANI nanocomposite for the detection of hydrazine, Mater Res Express 10 (2023). https://doi.org/10.1088/2053-1591/ad14c4.

[24] M. Raghasudha, D. Ravinder, P. Veerasomaiah, FTIR Studies and Dielectric Properties of Cr Substituted Cobalt Nano Ferrites Synthesized by Citrate-Gel Method, Nanoscience and Nanotechnology 3 (2013).

[25] D.R. Kumar, S.I. Ahmad, Ch.A. Lincoln, D. Ravinder, Structural, optical, room-temperature and low-temperature magnetic properties of Mg–Zn nanoferrite ceramics, Journal of Asian Ceramic Societies 7 (2019) 53–68. https://doi.org/10.1080/21870764.2018.1563036.

[26] A.K. Ambala, D.R. Kumar, S.I. Ahmad, K. Anuradha, C.A. Lincoln, Optical, luminescence and photocatalytic activity of Sr based Mg, Ce nano ferrites synthesized by citrate gel auto combustion method, Mater Today Proc 92 (2023) 801–806. https://doi.org/10.1016/J.MATPR.2023.04.346.

[27] P. Chand, S. Vaish, P. Kumar, Structural, optical and dielectric properties of transition metal (MFe2O4; M = Co, Ni and Zn) nanoferrites, Physica B Condens Matter 524 (2017) 53–63. https://doi.org/10.1016/J.PHYSB.2017.08.060.